



Document [NWPSAF-KN-UD-008](#)

Version 1.2

10-09-2018

High resolution data assimilation guide

Ad Stoffelen, Jur Vogelzang and Gert-Jan Marseille

KNMI, De Bilt, The Netherlands

High resolution data assimilation guide

Ad Stoffelen, Jur Vogelzang and Gert-Jan Marseille
KNMI, The Netherlands

This documentation was developed within the context of the EUMETSAT Satellite Application Facility on Numerical Weather Prediction (NWP SAF), under the Cooperation Agreement dated 29 June 2011 (CDOP2), between EUMETSAT and the Met Office, UK, by one or more partners within the NWP SAF. The partners in the NWP SAF CDOP2 were the Met Office, ECMWF, KNMI and Météo France.

Copyright 2018, EUMETSAT, All Rights Reserved.

Change record			
Version	Date	Author / changed by	Remarks
1.0	Jan 2012	Jur Vogelzang	First public release
1.1	Nov 2015	Jur Vogelzang	Changed layout
1.2	Sep 2018	Ad Stoffelen	In preparation NWP SAF wind data assimilation workshop

Contents

CONTENTS	3
1 INTRODUCTION.....	4
2 PRINCIPLES OF DATA ASSIMILATION.....	8
3 2DVAR AS DATA ASSIMILATION TEST BED.....	10
4 HOW TO IMPROVE THE ANALYSIS.....	15
5 THE PROBLEM OF MESOSCALE DATA ASSIMILATION	18
6 GUIDANCE.....	22
REFERENCES	24

1 Introduction

The purpose of data assimilation is to find a model state that gives the best match between the most recent model prediction and the observations that became available since. This state is called the analysis. It is the starting point for the Numerical Weather Prediction (NWP) model to calculate the forecasts. As computers become more powerful, more detailed NWP models are possible. As a consequence, this poses challenges not only to the model physics that should be able to describe meteorological features on smaller scales, but also to the observations that should ideally cover all scales of interest at sufficient temporal and spatial resolution and the data assimilation system that should produce a detailed analysis on the scales supported by the observations and the model.

Note that *Skamarock* (2006) identifies an important difference between NWP model resolution and grid sampling size; he suggests the effective NWP model resolution to be typically 5-10 times larger than the grid size. One may expect a similar effect in the vertical dimension due to dynamical closure (in the 3D turbulence regime). Global NWP models used for medium-range weather forecasting minimize model noise, i.e., they tend to only analyze atmospheric scales that are supported by the global observing system and thus may be analyzed deterministically. As a result, global NWP models lack convective-scale processes and for example do not show changing winds over the 50 min Metop-A and B time differences, whereas ASCAT observations show substantial changes near convection over large areas (100 km and more) (e.g., *King et al.*, 2017). Limitations in effective resolution provide a lower limit for the useful scale of flow we could attempt to derive from wind observations in global NWP. On the other hand, high resolution limited area models operate on the mesoscale and contain more small-scale variability. Some regional high-resolution NWP models (km scale grid) contain wind variability on the 10 km scale in the free atmosphere i.e. an order of magnitude smaller than global NWP models generally do. But since we do not have the observations to support the evolution of the fast 4D 10-km structures in a NWP model, we will have to deal with model noise on the unsupported scales.

How to determine the deterministic scales that observations may support? Although the km-scale regional models can resolve smaller scales in principle, these tend to change fast, and represent only modest energy conversion. Therefore, an extension of the observing system would be needed with spatially and temporally dense, very accurate and timely observations to initialize and evolve these scales in NWP models in a deterministic way. In fact, while some observation systems exist locally (e.g., descending aircraft near airports), the required quantity and coverage of observations remains a daunting challenge. In the absence of a resolving wind observing system to initialize

these turbulent scales in regional NWP models, high resolution NWP will face increased variances, faster changes and smaller scales in background error covariances. These changes potentially compromise the analysis of the larger scales. A trade-off between forecast horizon and short-term quality arises. We will discuss these challenges further in this report. A good understanding and analysis of effective model resolution and determined scales is anyway needed to proceed successfully.

Observations are lacking over sea, in the upper air, and in remote land areas, and do not support the analysis on the high resolution NWP model scales. In particular, on scales smaller than 500 km wind observations determine weather evolution, while these are generally lacking for mesoscale data assimilation. When strong surface forcing (e.g., orography) is absent and when model scales are not observed, and thus not analyzed, model noise will result. Model noise results in so-called “double penalties” in the data assimilation step and to detrimental effects in the forecasts due to error growth. In this report we provide a framework for discussion on how to optimally assimilate wind observations in 4D mesoscale data assimilation, taking account of considerations on observation density, accuracy, model resolution and the spatial scales involved.

In global NWP mainly the deterministic scales are analysed, which avoids the detrimental consequences of model noise on the medium range forecasts. We may use stable scatterometer winds to diagnose the evolution in σ - b over the past decade. Figure 1 shows the evolution of ASCAT and ECMWF mesoscale variances over the past decade. ASCAT variances are approximately constant, although a yearly cycle is evident in the world-wide ocean winds. The collocated ECMWF variances show the anticipated skill improvement over the years due to model improvements and the assimilation of more satellite data, leading to improved initial conditions and medium-range weather forecasts. About 10% of the mesoscale deficit of ECMWF winds with respect to ASCAT winds has been removed over the past decade, leading to a better verification of ECMWF winds (smaller σ - b). We expect that this gradual improvement will continue in the coming decades leading to a slow but gradual improvement in the mesoscale scales that can be deterministically tracked. On the other hand, this gradual progress will leave much room for regional mesoscale downscaling and data assimilation.

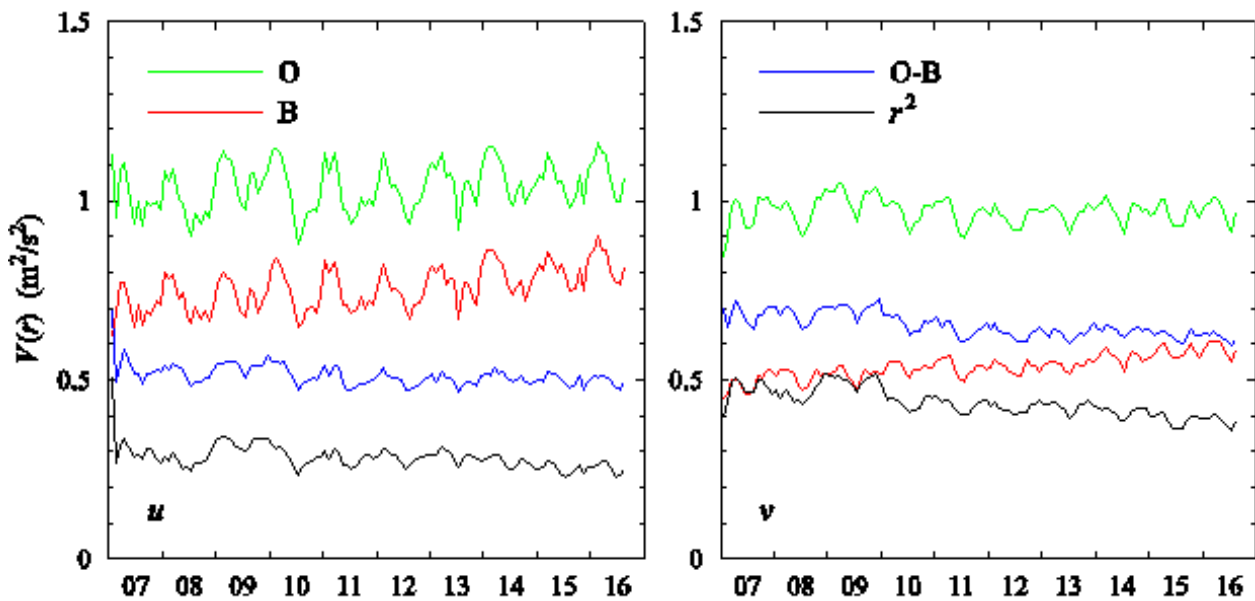


Figure 1 Variance in 25-km ASCAT winds (O) and collocated ECMWF data (B) below 200 km scales for the u (left) and v (right) components. O-B is the variance of the average difference between both and r^2 the variance present in ASCAT, but not in ECMWF fields.

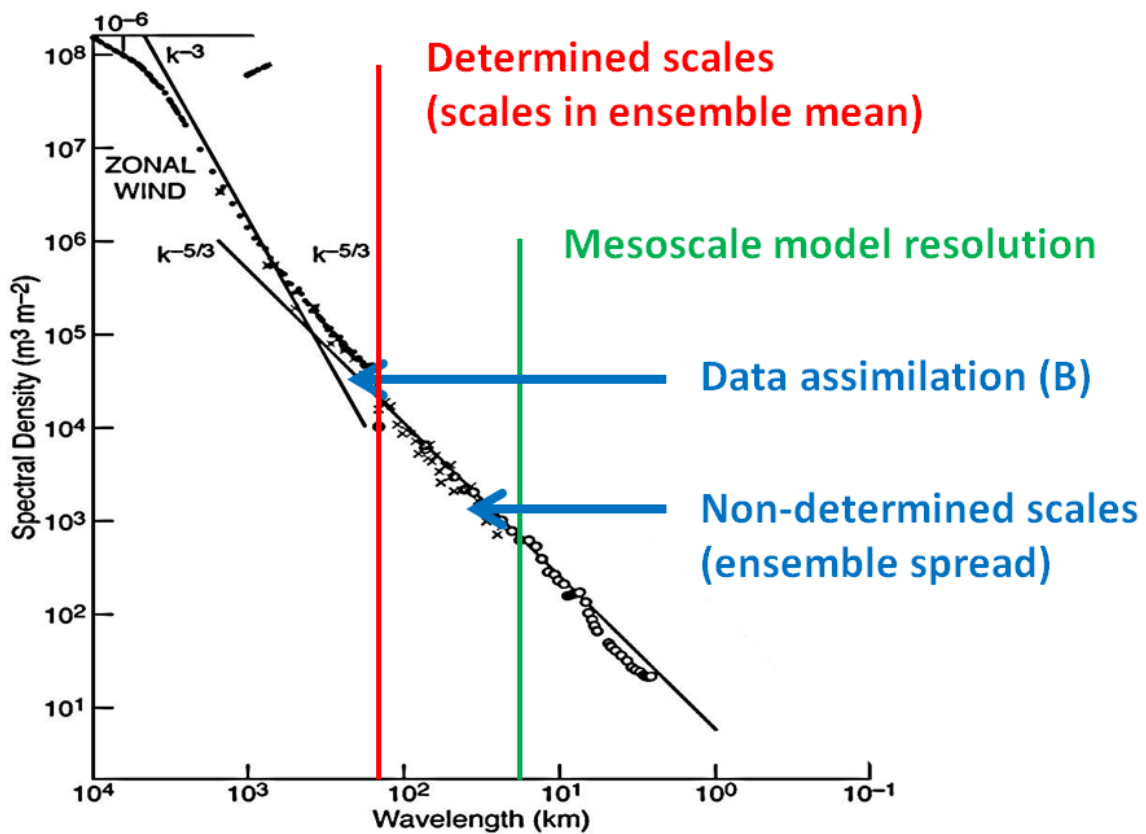


Figure 2 Mesoscale data assimilation, NWP model determined scales, non-determined scales or noise and the target area for scales updated in the analysis. Adopted from Nastrom and Gage (1987).

Figure 2 illustrates the above discussion and depicts the problem of mesoscale data assimilation schematically. The atmospheric transient flow is here broken down in different wave lengths, where fluid dynamics predicts 2D turbulence in the troposphere on the large (> 500km) synoptic scales, but 3D turbulence on the smaller mesoscales. In both regimes, the larger waves have the larger amplitudes, but this decay for increasing wavelength is fastest in the 2D turbulent regime. The set rate of amplitude decay in the 3D turbulence regime proves an excellent indicator of NWP model resolution, rather than the grid spacing, when compared to collocated observations. The smallest scales are thus the smallest in amplitude, but also the scales that evolve fastest, hence complicate NWP and nowcasting applications most. The report is intended for all who work on mesoscale data assimilation. The report is by no means exhaustive, nor will it answer all questions. In many cases only the challenges and caveats will be mentioned. User feedback is therefore more than welcome to keep this document up to date.

A closely related report from the EUMETSAT NWP SAF concerns model wind biases and how to prevent its detrimental effects in wind data assimilation (Document NWPSAF-KN-UD-007).

2 Principles of data assimilation

The data assimilation system¹ has the following components:

- Observation quality control,
- Analysis step, and
- Forecast step.

In the forecast step, using the previous analysis as initial conditions, a forecast model is run, which provides background information (the first guess) on the expected atmospheric state for the new observations in the next assimilation time window. The new observations will generally not perfectly agree with the background information, and in the analysis step both need to be compromised. If the accuracy of the observation is estimated to be poor, then the analysis will be close to the first guess. Conversely, when the observation is estimated to be very accurate as compared to the first guess, then the analysis will be close to the observation. The accuracies of the observations and the first guess are estimated on the basis of the monitoring of the differences between the first guess and the different observation types and parameters.

Lorenc (1988) describes common assumptions leading to 3D and 4D variational data assimilation and *Ide et al.* (1998) describe a detailed generic nomenclature used in data assimilation. The former author describes what is called “representativeness error” and which includes the variability in the different spatial, temporal and geophysical representation of the observations and the NWP model. *Vogelzang et al.* (2011) note that this representativeness error is spatially correlated for collocated buoy and scatterometer winds, since they measure the same true wind on scales between 25 km (scatterometer scale) and 150 km (ECMWF scale).

In 2015 *Lorenc* provided an excellent description of the different data assimilation techniques used and their benefits and limitations. An intricate part of data assimilation obviously exists in how observed information is used to inform (i.e., change) the NWP model state, where the background error covariances play a crucial role in the spatial and temporal filtering properties, i.e., to set the deterministic spatio-temporal scales of the NWP model error. On the other hand, also estimated error variances and observation density are crucial to determine the balance of weights between model-based and observed information. A too low weight of observations obviously minimizes impact, but too much observation weight may result in spurious analysis noise due to overfitting. We will further discuss this balance later on.

From statistical interpolation theory, see e.g. *Daley* (1998) the analysis state vector \mathbf{a} is given by

¹ MedEd tutorial: https://www.met.ed.ac.uk/training_module.php?id=704#.W5Uxif5IiiY

$$\mathbf{a} - \mathbf{b} = \mathbf{B}(\mathbf{B} + \mathbf{O})^{-1}(\mathbf{o} - \mathbf{b}) \quad (1)$$

with \mathbf{b} the background state vector, \mathbf{B} the background error covariance matrix, \mathbf{o} the observation state vector, and \mathbf{O} the observation error covariance matrix. In general, the observations are uncorrelated, so $\mathbf{O} = \sigma_o^2 \mathbf{I}$, with σ_o^2 the observation error variance and \mathbf{I} the identity matrix.

Such a data assimilation system acts like a filter (*Hollingsworth and Lönnerberg, 1986*). Suppose that \mathbf{e}_i is an eigenvector of \mathbf{B} with eigenvalue λ_i . Suppose further that $(\mathbf{a} - \mathbf{b})_i$ and $(\mathbf{o} - \mathbf{b})_i$ are the projections of $(\mathbf{a} - \mathbf{b})$ and $(\mathbf{o} - \mathbf{b})$ on \mathbf{e}_i . Then we have

$$\mathbf{B}(\mathbf{o} - \mathbf{b})_i = \lambda_i (\mathbf{o} - \mathbf{b})_i$$

$$(\mathbf{B} + \mathbf{O})(\mathbf{o} - \mathbf{b})_i = (\mathbf{B} + \sigma_o^2 \mathbf{I})(\mathbf{o} - \mathbf{b})_i = (\lambda_i + \sigma_o^2)(\mathbf{o} - \mathbf{b})_i$$


$$(\mathbf{B} + \mathbf{O})^{-1}(\mathbf{o} - \mathbf{b})_i = (\lambda_i + \sigma_o^2)^{-1}(\mathbf{o} - \mathbf{b})_i$$

and therefore

$$(\mathbf{a} - \mathbf{b})_i = \frac{\lambda_i}{\lambda_i + \sigma_o^2} (\mathbf{o} - \mathbf{b})_i \quad (2)$$

This implies that the data assimilation system acts as a low-pass filter with respect to the eigenvalues: eigenvectors of \mathbf{B} with eigenvalues larger than σ_o^2 are analyzed well, but those with eigenvalues smaller than σ_o^2 are suppressed in the analysis. The filter properties are thus determined by the estimated error covariances and the background error correlations, which in turn depend on the NWP model under consideration and the weather phenomena it describes.

The background error correlations are often parameterized, for example based on ensemble data assimilation. They are then referred to as structure functions. Note, however, that the term structure function is also used to denote correlations of spatial differences.

	<h2>High resolution data assimilation guide</h2>	Doc ID : NWPSAF-KN-UD-008 Version : 1.2 Date : 10-09-2018
---	--	---

3 2DVAR as data assimilation test bed

By the nature of the physical processes involved, wind measurements from a scatterometer are ambiguous, so additional information is needed to select the “best” ambiguity for a stand-alone wind product. This is called ambiguity removal. Various schemes have been proposed, and the KNMI scatterometer wind processors use 2DVAR, two-dimensional variational ambiguity removal (*Vogelzang et al., 2009*).

2DVAR consists of two steps:

- (1) Make an analysis from the scatterometer observations and an NWP background;
- (2) Select the ambiguity closest to the analysis (so 2DVAR could also be named “closest-to-analysis”) in order to prevent a substantial dependency on the background.

The analysis is made using the methods of statistical interpolation, and the first step of 2DVAR is very similar to 3DVAR or 4DVAR. Therefore 2DVAR can be used as a data assimilation test bed.

Figure 3 shows meridional wind component spectra of data in 2010 for ASCAT (red curves) at 25 km grid size and Mode-S (black curves) with the IFS-interpolated ECMWF background (dot-dashed). The blue line shows a $k^{-5/3}$ spectrum at arbitrary level. Such a spectrum is predicted in the atmosphere by Kolmogorov’s three-dimensional turbulence theory for scales smaller than about 500 km.

Figure 3 shows that the ECMWF background contains much less information than the ASCAT wind field at small and intermediate scales. This is mainly caused by the fact that the ECMWF model lacks detail in areas where valid scatterometer winds are measured and in the upper air above Europe at the Mode-S tracks. We note that the 2DVAR analysis follows the background and fails to incorporate the small scale information in the ASCAT measurements. This is a consequence of the filtering properties of 2DVAR, with small eigenvalues corresponding with eigenvectors that describe small detail.

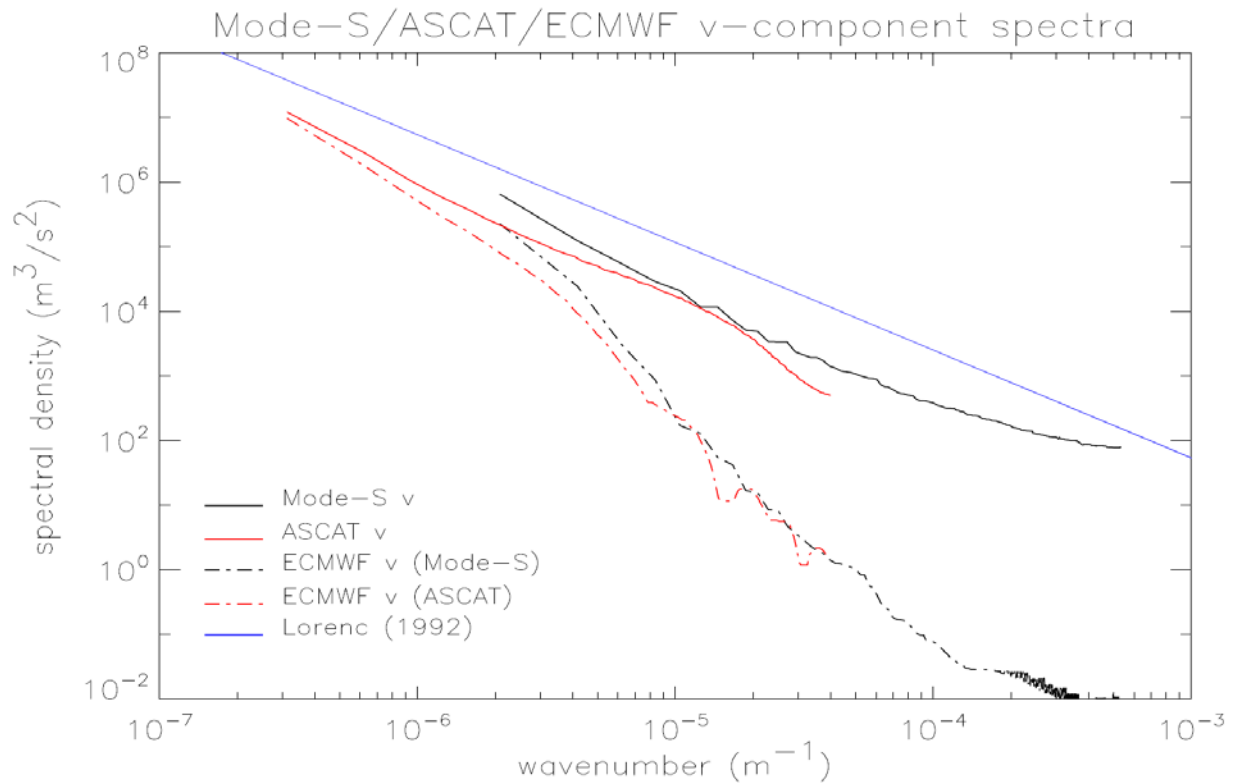


Figure 3 Wind component spectra of ASCAT-12.5km 10-m winds, Mode-S aircraft winds at 10 km height and collocated ECMWF winds at both 10 m for ASCAT and 10 km for Mode-S over 2010.

2DVAR contains a number of parameters: the error variances of observations and background and the structure function parameters. The error variances are estimated by triple collocation (Vogelzang *et al.*, 2011). As an example Figure 4 shows an ASCAT wind field on a 25 km grid on 17 November 2009 around 17:40 UT obtained with the default 2DVAR settings. Figure 5 shows the same area, but now with the structure function cut-off reduced to 100 km. As a consequence, ambiguity removal errors are visible in the northwestern part of the wind field.

Apparently, the short-ranged structure functions are not able to describe the inflow to the cyclone. The reason for this error is shown in Figure 6: a spurious developing low near 25°S and 120°W. This example illustrates that mesoscale model errors in combination with mesoscale structure functions may be quite detrimental for 2DVAR and for meteorological analysis more in general.

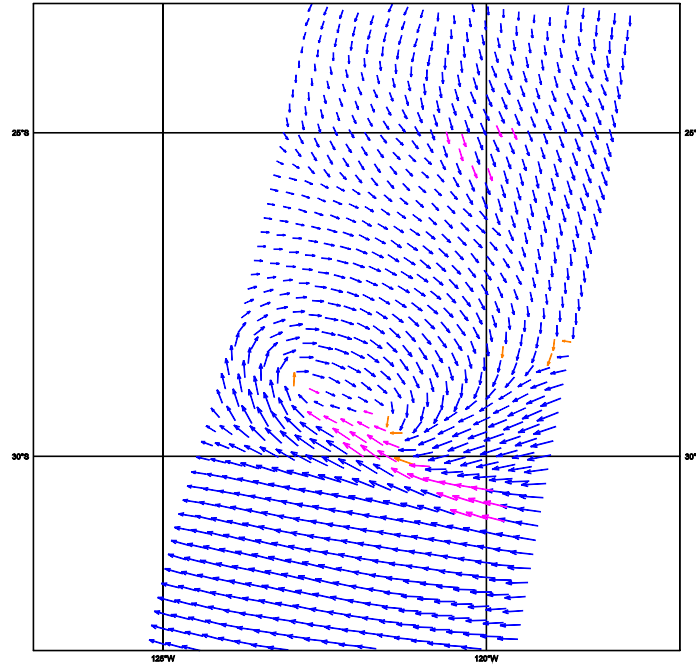


Figure 4 ASCAT-25 wind field on 17-11-2009 around 17:40 UT in the Southern Pacific. Purple arrows indicate cells that have the variational quality control set, orange arrows cells that have the MLE quality control set.

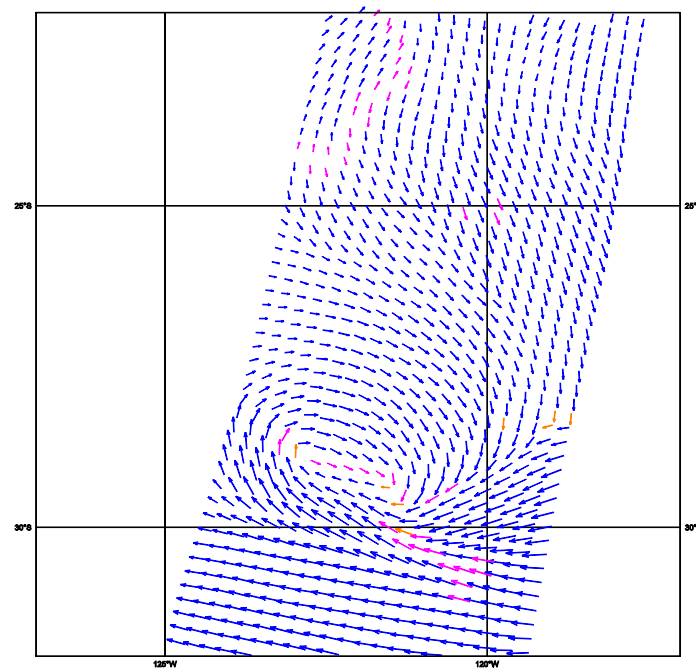


Figure 5 As Figure 4, but obtained with a structure function cut-off of 100 km.

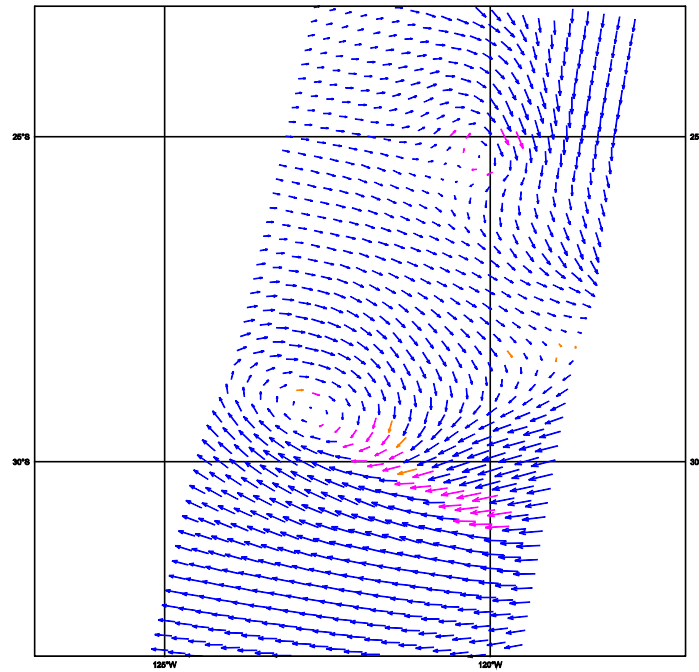


Figure 6 Background belonging to Figure 4 and Figure 5.

Background error covariances are analyzed at ECMWF using an ensemble of data assimilations (*Isaksen et al., 2010*). *Lin et al. (2015)* used ASCAT and triple collocation in categories of wind variability to verify the model-simulated ensemble background error covariances. It appears that local wind variability is an excellent indicator of background model error and reliable spatial maps of background error covariance may be produced based on the ASCAT data, as in Figure 7.

We note from Figure 7 that background error covariances have substantial mesoscale variability, while the modelled covariances are on the synoptic scale. Nevertheless, areas of enhanced error covariances largely overlap in the left swath, while these areas are poorly correlated in the right swath in the plot. We note that the more relevant quantity of the estimated ratio b to o error has the same spatial patterns, but is somewhat moderated in amplitude due to the fact that the estimated observation error covariance also somewhat increases with increased local wind variability. Note that ECMWF, like many other data assimilation centers, assumes the estimated observation error covariances to be constant for simplicity.

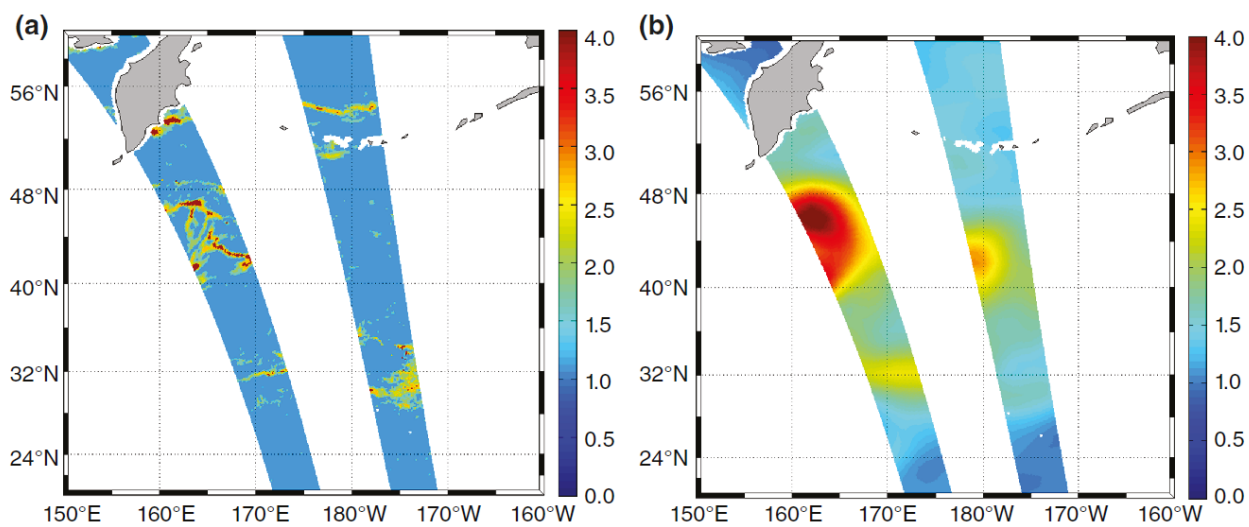


Figure 7 (a) Estimated ECMWF background wind errors from ASCAT L2 data, 3 January 2013, around 0900 UTC, (b) the collocated EDA background errors. The color bars are in m s^{-1} (from *Lin et al., 2016*). (c) RMets 2016.

4 How to improve the analysis

In order to assimilate mesoscale features into a NWP model, one should use realistic values for the error variances and structure functions. Error variances of observations and background may be found using triple collocation (*Vogelzang et al., 2011*). Fitting structure functions may be obtained from ASCAT observations as these have excellent spatial sampling and no error correlations on the NWP model scale (*Vogelzang and Stoffelen, 2017*). Spatial **o-b** difference structures may thus be attributed to background error correlation in the following way: In the homogeneous and isotropic case the error autocorrelations for the longitudinal and transversal wind components, ρ_{ll} and ρ_{tt} , read (*Daley, 1998*)

$$\rho_{ll}(r) = -L_{\psi}^2 (1 - \nu^2) \frac{1}{r} \frac{d\rho_{\psi\psi}(r)}{dr} - L_{\chi}^2 \nu^2 \frac{d^2 \rho_{\chi\chi}(r)}{dr^2} \quad (3a)$$

$$\rho_{tt}(r) = -L_{\psi}^2 (1 - \nu^2) \frac{d^2 \rho_{\psi\psi}(r)}{dr^2} - L_{\chi}^2 \nu^2 \frac{1}{r} \frac{d\rho_{\chi\chi}(r)}{dr} \quad (3b)$$

with $\rho_{\psi\psi}$ and $\rho_{\chi\chi}$ the autocorrelations of the stream function and velocity potential. L_{ψ} and L_{χ} are length scales, and ν^2 is the divergence/rotation ratio. ρ_{ll} and ρ_{tt} are observables, while $\rho_{\psi\psi}$ and $\rho_{\chi\chi}$ are the structure functions that make up the background error covariance matrix. *Vogelzang and Stoffelen [2011]* show how equations (3a-b) can be solved for $\rho_{\psi\psi}$ and $\rho_{\chi\chi}$. In the case of 2DVAR, this procedure leads to velocity potential and stream function structure functions with a long range, but to wind velocity increments with a short range that support mesoscale analysis.

Figure 8 shows the impact of the numerical structure functions as the spectral ratio of the resulting analysis with the default analysis as a function of $s=1/k$. Indeed application of numerical structure functions increases the information content of the analysis at small and intermediate scales considerably: up to a factor of 6 for ν at scales around 150 km. Indeed, collocated spectra of **b**, **a** and **o** show that the structure functions obtained from **o** are able to elevate the **a** spectra above the **b** spectra and towards the **o** spectra on scales of a few hundred kms (*Lin et al., 2016*).

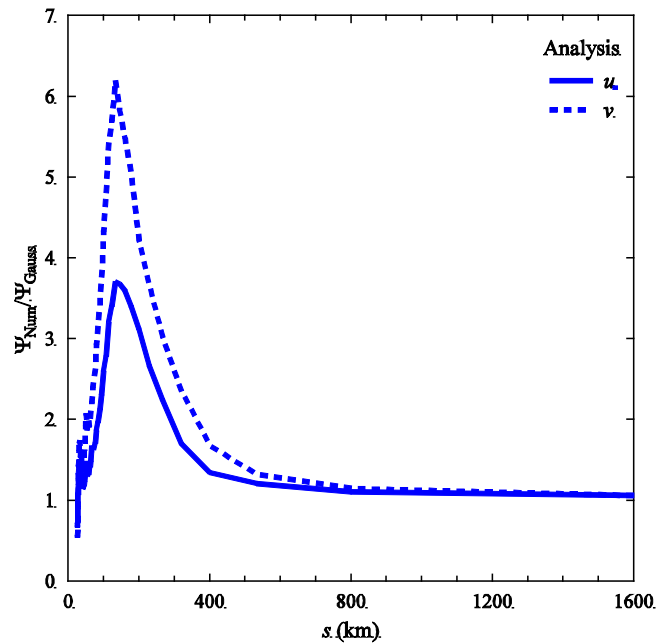


Figure 8 Spectral ratio of analysis increment amplitudes obtained with numerical structure functions based on ASCAT *o-b* and amplitudes based on the default Gaussian structure functions..

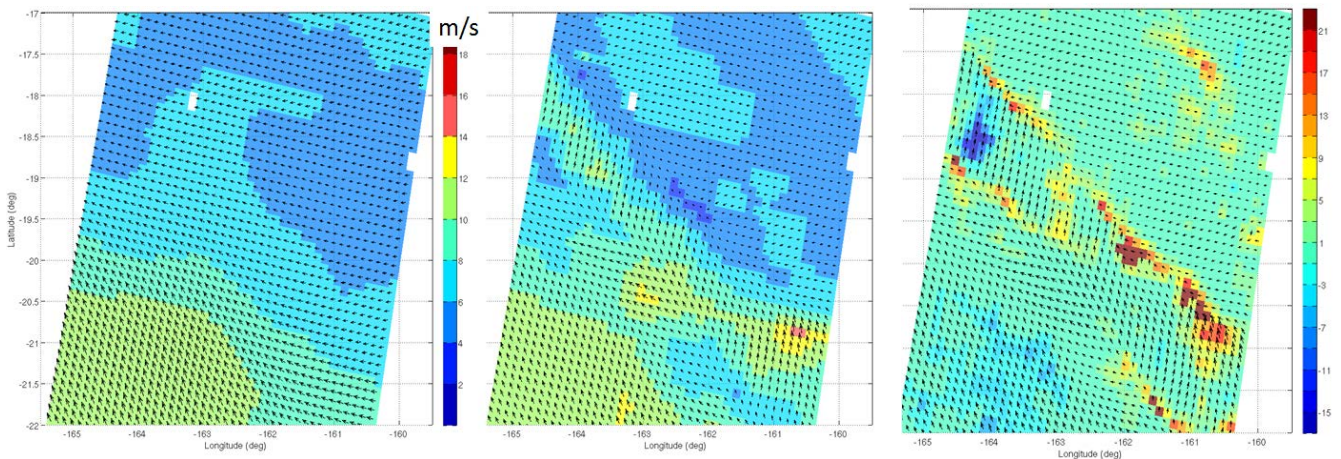



Figure 9 2DVAR analysis fields obtained with default background error covariances (left) and ASCAT-based numerical ones (middle), with corresponding selected ASCAT wind field (right). The color legend for the left and middle plot provides wind speed in m s⁻¹, while for the right plot the retrieval residual is shown in multiples of the mean standard deviation, where negative (positive) values indicate stable (variable) flow.

Figure 9 shows a typical case of the default and updated 2DVAR analysis fields, where the enhanced information content by using the ASCAT-based background error covariances is evident. The right panel shows that areas of stable flow are divided by areas of variable flow, which

	<h2>High resolution data assimilation guide</h2>	Doc ID : NWPSAF-KN-UD-008 Version : 1.2 Date : 10-09-2018
---	--	---

generally appear near convection, lows, squall lines or fronts. These are now better visible in the middle 2DVAR analysis.

The background error structure functions obtained from ASCAT were also applied to 2DVAR for pencil-beam scatterometers, confirming their suitable and beneficial spatial filtering properties (*Vogelzang and Stoffelen, 2018*).

Last, but not least, we note that conceptual differences between 2DVAR and 4D-var may not be large, but their practical use and objectives are slightly different. In this case, mesoscales are added to **b** in order to fit the scatterometer winds and thus improve ambiguity selection, resulting in a more complete mesoscale wind energy spectrum in **a**. However, the energy density spectrum of **b** is governed by the dynamical closure of the NWP model, which implies that enhanced variability in **a** will be filtered out by the forward model equations in only a few model time steps (*Skamarock, 2004*). As such, in mesoscale data assimilation, it is crucial that observations are assimilated in the NWP model space representation. A second difference is that observation weights may be increased in 2DVAR to closely fit the scatterometer winds, since our interest is solely to improve the analysis for ambiguity selection. Using the same weights in 3D- or 4D-var may lead to overfitting artefacts outside the scatterometer swath and in the upper air, leading potentially to dynamical unbalance. This should obviously be prevented at all times and local or average analysis impact structure may be inspected to diagnose for such detrimental effects.

5 The problem of mesoscale data assimilation

Figure 2 depicts NWP mesoscale wind data assimilation. Figure 3 shows that 3D turbulence is not well represented in global NWP; the figure shows horizontal scales, but also vertical scales are lacking (*Houchi et al., 2010*) as expected for 3D flow. Mesoscale modelling usually starts with dynamically downscaled global NWP fields and soon after spinning the NWP model up, enhanced mesoscale variability will appear. *Winterfeldt et al. (2011)* verified the difference between the downscaled fields and the input global NWP field with QuikSCAT winds over sea as shown in Figure 10.

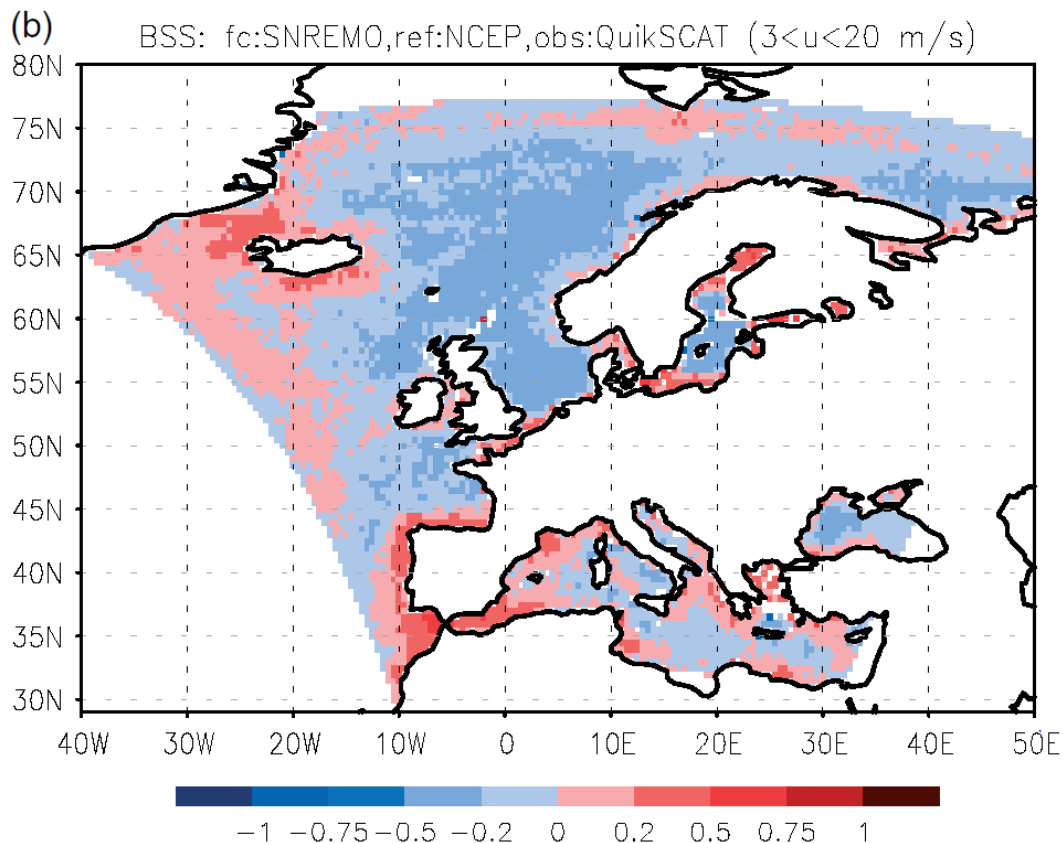


Figure 10 Differences global minus downscaled of variances obtained by verifying the fields with QuikScat winds. The color represents the local value normalized by the largest variance of model fields minus QuikScat. Oceans are blue implying noise generation by dynamical downscaling (from *Winterfeldt et al., 2011*). © RMets

The dynamically downscaled variance indeed degrades the verification with QuikSCAT over open sea, even though the downscales fields in principle better resolve the 3D turbulent scales observed by QuikScat. Seemingly, the generated scales are meteorologically colored noise rather than real variability. This comes as no surprise as there is no physical forcing over open sea to lock

the turbulent scales and the generated mesoscale variability will be random. Near orography and coastal areas more in general, dynamically downscaled variability appears more truthful, as expected, as orographic flow and land-sea breezes are better resolved. To capture the amplitude of the model noise, ensemble data assimilation systems have been devised, that naturally distinguish the determined variance (ensemble mean) from the undetermined variance (ensemble spread). Model noise contributes to $o-b$ differences and thus affects analysis quality.

As an example, *Marseille and Stoffelen (2017)* tested $o-b$ versus spatial aggregation of the mesoscale model state, in this case HARMONIE. They used scatterometer data from the Chinese HY-2A scatterometer, HSCAT, processed to 50-km sampled winds at KNMI. The HARMONIE effective horizontal resolution was diagnosed to be ~ 25 km at a grid distance of grid 2.5 km. The $o-b$ wind component difference is excessively large without temporal interpolation and the need and expected benefit of temporal interpolation was thus confirmed. With adequate temporal and spatial interpolation through the so-called observation operator, the $o-b$ (u, v) wind component standard deviation amounted to (1.36, 1.29), while after averaging the model state to the HSCAT samples at 50 km size, it reduced to (1.25, 1.18), which amounts to a reduction of 16% in the $o-b$ vector difference. The standard deviation of $o-b$ (u, v) differences of HSCAT with respect to ECMWF (6-hour forecast) amounts to (1.09, 1.18), or a 27% reduction with respect to HARMONIE at full resolution. As shown in Figure 3 the ECMWF model resolution is ~ 150 km over the open ocean and almost equal to the deterministic resolution, conform Figure 2. Obviously, a smaller $o-b$ may result in a better analysis when it is used as an innovation to inform the deterministic model state.

We may write

$$o = t + \varepsilon_O + \varepsilon_R \tag{4}$$

$$b = t + \varepsilon_D + \varepsilon_N \tag{5}$$

with t defined as the truth on deterministic scales. ε_O is defined as the observation error on the scale of the model resolution and ε_R is the true variance on the scales of the model noise (see Figure 2). ε_D is the model error on the deterministic scales and ε_N the model noise. By definition, the errors and the truth on the different scales are independent, i.e., $\langle t\varepsilon_O \rangle = \langle t\varepsilon_R \rangle = \langle \varepsilon_O \varepsilon_R \rangle = 0$, $\langle t\varepsilon_D \rangle = \langle t\varepsilon_N \rangle = \langle \varepsilon_D \varepsilon_N \rangle = 0$. Then

$$\langle (o - b)^2 \rangle = \sigma_O^2 + \sigma_D^2 + \sigma_R^2 + \sigma_N^2 \tag{6}$$

where all errors ε in eqs. (4-5) have expected standard deviation σ . Further, $\langle \varepsilon_O \varepsilon_D \rangle = \langle \varepsilon_O \varepsilon_N \rangle = 0$ and $\langle \varepsilon_R \varepsilon_D \rangle = \langle \varepsilon_R \varepsilon_N \rangle = 0$, since the latter errors are true variance and synthetic model variance

(noise), while the former errors are each on different scales and thus not correlated. Finally, the weight W determines the analysis increments in this simplified equation at observation positions

$$a - b = W(o - b) \quad (7)$$

Following eq. (6) a will thus be effected by model noise ε_N , observation representation error ε_R , observation error ε_O , and model error ε_D . We note that both ε_R and ε_N contribute to the difference $o-b$, but where these are really defined as wind variability on the same scales. Their contributions to $o-b$ present a so-called double penalty, while the analysis should not target these scales as these cannot be well determined. In other words, $o-b$ does not only inform the (to be) determined dynamical scales targeted by the analysis, but also includes a double penalty.

Observations need to be accurate and well resolved for mesoscale data assimilation and they may be better used in mesoscale NWP data assimilation in principle. However, some complications arise. Following conventional logic, one may be tempted to assimilate scatterometer winds at full resolution in a mesoscale data assimilation system. This would imply a scatterometer wind component error of about 0.8 m/s (*Vogelzang et al., 2011*). In addition, model noise variance (see above) would need to be added to the \mathbf{B} matrix, which makes the background error covariances larger and more pronounced on the smaller scales. This is, the weight of the observations would be much increased, while the weight of the background is reduced. Moreover, the scale of the \mathbf{B} error correlations is reduced, allowing more small scales to be informed in the analysis step, i.e., small scales that cannot be fully determined (see paragraph below). The addition of uncertain small scales in the analysis moreover will go at the expense of informing the larger scales well. Uncertain \mathbf{B} in case of small observation error leads to analysis updates above or close to the observations that are unrealistic and often denoted as overfitting, caused by inaccurate and high innovation weights. Overfitting is known to lead to so-called spin-up that essentially represents a dynamical interference with the information brought by the new observations in the analysis step, which latter information is then lost in further model noise generation.

4D structures that cannot be determined, but are part of the analysis will result in deformed dynamical structures. This problem is called “aliasing”² in engineering and *Nyquist (1928)* formulated a criterion to prevent aliasing, which is oversampling by a factor of two in all dimensions to prevent the generation of artificial waves (Moiré effect). The problem applies to meteorological analysis and is potentially aggravated by the dynamical development of these artificial waves in the high-resolution NWP model.

² https://en.wikipedia.org/wiki/Nyquist-Shannon_sampling_theorem

How to prevent artificial dynamical waves? 3D turbulence potentially requires both horizontal and vertical sampling of structures to prevent aliasing. Moreover, time sampling may provide an additional observation constraint. Background error covariances are used to spatially project observed information, while 4D-var has a capability to fit observed temporal tendencies. These capabilities contribute to extending the determined scales to smaller wavelength. Fully optimized capability of these aspects at ECMWF leads to a deterministic resolution in the dynamically constrained areas over sea and in the upper air of about 150 km (see Figure 3). Over some land areas, more and accurate upper air wind profile observations may become available from airplanes, such that smaller 4D scales may be determined (*de Haan and Stoffelen, 2012*), but likely not at the rate of model resolution improvements in NWP. Therefore, the problem of model noise in data assimilation will be aggravated in the future. How could mesoscale models do better? Given the above, we could only do better (locally) if we assimilated more spatially and temporally dense (wind) observations and if we overcome the problem of mesoscale model noise in the data assimilation step.

Ensemble data assimilation encapsulates the concept of model noise and of the deterministic scales that are represented in the ensemble mean. This is, when the data assimilation ensemble would be sufficiently large to fully represent the model noise distribution and when the ensemble represents the model noise well, i.e., is run at full resolution. Given the expense of ensemble data assimilation, both conditions are usually not met. Moreover, each ensemble member is dealing with the double penalty in $o-b$ and does not provide the best possible deterministic state. As a result, the shared true variance in the ensemble mean will be compromised.

6 Guidance

In this report we sketch a new paradigm for mesoscale wind data assimilation. It is motivated by the substantial variability on the fast mesoscales in the 3D turbulence regime and the lack of mesoscale observations to appropriately capture fast small-amplitude 4D structures. In this final chapter we provide guidance based on the content of the earlier chapters.

Background error covariances are difficult to estimate. State-of-the-art methods use 4D-var and adaptive \mathbf{B} covariances based on an ensemble of data assimilation in global NWP (EDA); see Figure 7. In global NWP, the deterministic scale is generally quite close to the model resolution (cf. Figure 3) and innovations are thus projected onto the deterministic scales. Background error variances may be statistically correct, but in any situation do not well represent the actual spatio-temporal structure of the real errors. Of course, if we knew these latter, we would not be writing this guidance report! Nevertheless, it is important to realize that the difference between estimated background error covariances and the actual model errors dominates the quality of an analysis. Following Figure 2 we suggest to project the innovations onto those scales that can be determined, which somehow excludes the scales where mesoscale model noise dominates. If model noise is represented in \mathbf{B} , then the innovation $o-b$ would be projected onto those noisy scales, which would likely result in rather artificial dynamical structures (aliasing) and less of the innovation would be projected onto the larger deterministic scales (see section 5).

Model noise is however captured in b which is propagated into analysis noise too for every (ensemble) analysis, as elaborated in section 5. How can we prevent this? We may consider averaging the model state to reduce model noise and thus prevent a double penalty in data assimilation. This may be done while interpolating the model state to the observed location. Following the logic of Nyquist, we would average up to half the distance of the deterministic resolution, i.e., typically 100 km over sea and in the upper air. In analogy to “superobbing”, we may call this “supermodding”. It would much reduce σ_N in equation 6.

To reduce σ_R in equation (6) superobbing may be applied, in addition to supermodding, up to half of the deterministic resolution. Extending the approach of *Marseille and Stoffelen (2017)* one may be tempted to spatially average o and b until we minimize $o-b$. Following equation (6) $o-b$ may be reduced by reducing one of four terms, including σ_D . However, reducing σ_D is not a good thing at all, since the deterministic scales include true observed and, importantly, true model variance. A better approach will be to diagnose all of $o-b$, b and o variance reductions while averaging b to b_A on the deterministic scales

$$\langle b_A^2 \rangle = \sigma_T^2 + \sigma_D^2 \tag{8}$$

$$\langle b_A^2 \rangle - \langle (o - b_A)^2 \rangle = \sigma_T^2 - \sigma_O^2 - \sigma_R^2 \tag{9}$$

$$\langle b^2 \rangle - \langle (o - b)^2 \rangle = \sigma_T^2 - \sigma_O^2 - \sigma_R^2 \tag{10}$$

where σ_T^2 corresponds to the true variance in the deterministic scales or, practically, common scales between observations and background. As long as averaging cancels only part of σ_N^2 and σ_R^2 , the variance in (9) and (10) remains the same. As soon as true common variance is averaged out in b the difference in (9) will be reduced. The difference $\langle o_A^2 \rangle - \langle (o_A - b)^2 \rangle$ has similar properties and may be diagnosed at the same time for different averaging lengths in case the observations are spatially dense (superobbing).

In Figure 3 aircraft winds are provided at flight level. Note that vertical averaging over 1 km will typically imply wind changes of 4 m s^{-1} , as this is the mean atmospheric vertical wind shear (*Houchi et al., 2010*) and 1-km vertical variance corresponds to a horizontal variance over 100 km as the horizontal/vertical aspect ratio of 3D turbulence is typically 100 (*Nastrom and Gage, 1985*).

Supermodding may be implemented in the background interpolation operator in data assimilation, where the horizontal/vertical model space context should a priori be made available to the computer processor working on the observation innovation for efficient implementation.

As stated earlier, a smooth **B**, supermodding and superobbing up to the deterministic dynamical scales would also improve ensemble data assimilation, due to the avoidance of a double penalty in the model noise regime.

References

- Daley, R., 1998, *Meteorological data analysis*. Cambridge University Press.
- Hollingsworth, A., and P. Lönnberg, 1986, The statistical structure of short-range forecast errors as determined from radiosonde data. Part I: The wind field. *Tellus*, **38A**, 111-136.
- Houchi, K., A. Stoffelen, G.J. Marseille and J. de Kloe, 2010, Comparison of wind and wind shear climatologies derived from high-resolution radiosondes and the ECMWF model, *J. Geophys. Res.*, D, 2010, 115, 22123, doi:10.1029/2009JD013196.
- Ide, Kayo, Courtier, Philippe, Ghil, Michael, Lorenc, Andrew C, 1997, "Unified Notation for Data Assimilation: Operational, Sequential and Variational", (Special Issue:Data Assimilation in Meteorology and Oceanography: Theory and Practice) *Journal of the Meteorological Society of Japan. Ser. II*. 75 (1B): 181–9. doi:10.2151/jmsj1965.75.1B_181.
- Isaksen, L., M. Bonavita, R. Buizza, M. Fisher, J. Haseler, M. Leutbecher, L. Raynaud, 2010, Ensemble of data assimilations at ECMWF, Technical memorandum 636, ECMWF, Reading UK, <https://www.ecmwf.int/en/elibrary/10125-ensemble-data-assimilations-ecmwf>.
- Lin, Wenming, Marcos Portabella, Ad Stoffelen, Jur Vogelzang and Anton Verhoef, 2016, On mesoscale analysis and ASCAT ambiguity removal, *Q. J. R. Meteorol. Soc.* 142: 1745–1756, B, DOI:10.1002/qj.2770.
- Lorenc, Andrew C., 2015, Advances in data assimilation techniques and their relevance to satellite data assimilation, ECMWF seminar, <https://www.ecmwf.int/sites/default/files/elibrary/2015/10811-advances-data-assimilation-techniques-and-their-relevance-satellite-data-assimilation.pdf>.
- Lorenc, Andrew C., 1988, Optimal nonlinear objective analysis. *Q. J. R. Meteorol. Soc.* 114: 205–240, doi:http://dx.doi.org/10.1002/qj.49711447911.
- Marseille, G.-J., and A. Stoffelen, 2017, "Toward Scatterometer Winds Assimilation in the Mesoscale HARMONIE Model", *IEEE J. Sel. Topics in Appl. Earth Observ. and Rem. Sensing* 10(5), 2383-2393, doi: 10.1109/JSTARS.2016.2640339.
- Nastrom, G.D. and K.S. Gage, 1985, A Climatology of Atmospheric Wavenumber Spectra of Wind and Temperature Observed by Commercial Aircraft. *J. Atmos. Sci.*, 42, 950–960, [https://doi.org/10.1175/1520-0469\(1985\)042<0950:ACOWS>2.0.CO;2](https://doi.org/10.1175/1520-0469(1985)042<0950:ACOWS>2.0.CO;2)
- Nyquist, Harry, 1928, "Certain topics in telegraph transmission theory", *Trans. AIEE.* 47: 617–644, doi:10.1109/t-aiee.1928.5055024. Reprint as classic paper in: *Proc. IEEE* 90(2), 2002.
- Skamarock ,William C., 2004, Evaluating Mesoscale NWP Models Using Kinetic Energy Spectra, *Monthly Weather Review* 134, 3019-3032, <https://doi.org/10.1175/MWR2830.1>.
- Vogelzang, J., A. Stoffelen, A. Verhoef, J. de Vries, and H. Bonekamp, 2009, Validation of two-dimensional variational ambiguity removal on SeaWinds scatterometer data. *J. Atm. Ocean. Engin.*,
- Vogelzang, J., A. Stoffelen, A. Verhoef, and J. Figa-Saldaña, 2011, On the quality of high resolution scatterometer winds. *J. Geophys. Res.*,
- Vogelzang. J., and A. Stoffelen, 2011, NWP model error structure functions obtained from scatterometer winds. *IEEE Trans. Geosci. Rem. Sens.*,

Vogelzang, J., and A. Stoffelen, 2017, "ASCAT Ultrahigh-Resolution Wind Products on Optimized Grids", IEEE Journal of Selected Topics in Applied Earth Observations and Remote Sensing , vol.10, no.5, pp. 2332-2339, doi: 10.1109/JSTARS.2016.2623861.

Vogelzang, J., and A. Stoffelen, 2018, "Improvements in Ku-band scatterometer wind ambiguity removal using ASCAT-based empirical background error correlations", Quarterly Journal of the Royal Meteorological Society, accepted, DOI: 10.1002/qj.3349.

Winterfeldt, Jorg., Beate Geyer and Ralf Weisse, 2011, Using QuikSCAT in the added value assessment of dynamically downscaled wind speed, Int. J. of Climatology 31, 1028–1039, DOI: 10.1002/joc.2105.